Temperature-dependent photocarrier recombination dynamics in Cu2ZnSnS4 single crystals

Le Quang Phuong, Makoto Okano, Yasuhiro Yamada, Akira Nagaoka, Kenji Yoshino, and Yoshihiko Kanemitsu

Citation: Applied Physics Letters **104**, 081907 (2014); doi: 10.1063/1.4866666
View online: http://dx.doi.org/10.1063/1.4866666
View Table of Contents: http://scitation.aip.org/content/aip/journal/apl/104/8?ver=pdfcov
Published by the AIP Publishing

Temperature-dependent photocarrier recombination dynamics in Cu_2ZnSnS_4 single crystals

Le Quang Phuong,[1,2] Makoto Okano,[1] Yasuhiro Yamada,[1] Akira Nagaoka,[3] Kenji Yoshino,[3] and Yoshihiko Kanemitsu[1,2,a)]
[1]*Institute for Chemical Research, Kyoto University, Uji, Kyoto 611-0011, Japan*
[2]*Japan Science and Technology Agency, CREST, Uji, Kyoto 611-0011, Japan*
[3]*Department of Applied Physics and Electronic Engineering, University of Miyazaki, Miyazaki 889-2192, Japan*

(Received 18 December 2013; accepted 11 February 2014; published online 24 February 2014)

Time-resolved photoluminescence (PL) measurements have been used to study the temperature-dependent photocarrier recombination dynamics in Cu_2ZnSnS_4 (CZTS) single crystals. We found a significant change of nearly four orders of magnitude of the PL decay time, from microseconds at low temperatures to subnanoseconds at room temperature. The slow PL decay at low temperatures indicates localization of the photocarriers at the band tails. Due to the large band tail states, the PL decay time depends strongly on both the photon energy and excitation density. It is pointed out that the drastically enhanced nonradiative recombination at high temperatures is one of the main factors that determine the power conversion efficiency of CZTS-based solar cells.
 [http://dx.doi.org/10.1063/1.4866666]

The earth-abundant quaternary compound Cu_2ZnSnS_4 (CZTS) is recently considered to be one of the most promising light absorbers for next-generation low-cost thin-film solar cells because of its optimal band-gap energy for solar energy conversion and high absorption coefficients in the near-infrared and visible spectral regions.[1–3] However, CZTS-based solar cells are reported to have a relatively low power conversion efficiency of ~8.4% (maximum)[4] that is believed to be primarily due to intrinsic defects in the quaternary compound CZTS.[5–8] Several studies devoted to the roles of the defects in the electrical and optical responses of CZTS have resulted in several defect-state-related photocarrier recombination models given in terms of donor-acceptor pair (DAP) recombination,[9,10] quasi-DAP recombination,[11] free-to-bound transitions,[12] and a potential fluctuation model[3,13–16] based mainly on steady-state photoluminescence (PL) measurements. A recent dynamical study revealed the significant role of the band tail states at room temperature (RT); rapid localization of photocarriers occurs in the band tail states just after photoexcitation.[3] Time-resolved optical spectroscopy,[17] therefore, is essential for obtaining more insights into the optical response of new solar-cell materials such as CZTS.

The temperature dependence of the PL dynamical properties provides crucial information for understanding photocarrier recombination mechanisms, which determine the performance of CZTS-based solar cells. Moreover, fundamental physical knowledge of the temperature dependence of the optical response of the CZTS absorber is important for particular practical CZTS-based solar-cell applications in, for example, the aerospace industry. To date, investigations of the dynamical behavior of photogenerated carriers have been restricted to $Cu_2ZnSn(S,Se)_4$-based solar devices at very limited temperatures: RT and 4 K.[11,16] Thus, both temperature-dependent and time-resolved optical studies are expected to provide further insights into the photon energy conversion processes in CZTS.

In this Letter, we clarify the temperature dependence of the photocarrier recombination dynamics in CZTS single crystals based on a combination of experimental results obtained from simultaneous steady-state and time-resolved PL measurements. We found that long-lived microsecond localization of the photocarriers at the band tails determines the optical response of the CZTS single crystals at low temperatures, whereas drastically enhanced nonradiative recombination plays a significant role in the photocarrier recombination dynamics as the temperature increases. The strong temperature, PL-photon-energy, and excitation-density dependences of the PL decay time indicate the existence of large band tails in the CZTS single crystals, which in turn determines the power conversion efficiency of CZTS-based solar cells.

The CZTS single crystals investigated in this study were grown using the traveling heating method.[18] The single-crystal composition was estimated from the stoichiometric ratio to be slightly Cu-poor, Zn-rich, Sn-poor, and S-rich; a composition that is believed to be important for obtaining highly efficient CZTS-based solar cells.[4,19] The as-grown CZTS single crystals with a typical size of $5 \times 3 \times 1.5$ mm^3 were mounted onto the cold finger of a He-flow-type cryostat, and temperature dependent measurements were conducted while the sample temperature was changed from 10 K to RT.

In the simultaneous steady-state and time-resolved PL measurements, an excitation pulse emitted from an optical parametric amplifier pumped by a Yb:KGW (potassium gadolinium tungstate) regenerative amplified laser with a pulse duration of ~300 fs and a repetition rate of 100 kHz was focused onto the surface of the sample to a spot size of

a)Author to whom correspondence should be addressed. Electronic mail: kanemitu@scl.kyoto-u.ac.jp

$\sim$100 μm as measured by a beam profiler. The excitation photon energy was tuned to 2.08 eV, which is well above the band-gap energy of CZTS estimated to be about 1.58 eV.[3] The PL signal was collected in the backward configuration and directed onto the entrance slit of a 50-cm monochromator equipped with a liquid-nitrogen-cooled Si charge-coupled-device camera. The spectral responses of all the PL measurements were calibrated using a standard lamp. The time-resolved PL measurements were performed using a near-infrared streak camera and a monochromator. The temporal resolution of our system was about 20 ps. For the PL excitation (PLE) measurements, a wavelength-tunable continuous-wave Ti:sapphire laser was used as the excitation source with the excitation photon energy tuned from $\sim$1.33 to $\sim$1.72 eV. The PL signal was detected by a liquid-nitrogen-cooled InGaAs photodiode array through a 30-cm monochromator.

Figure 1(a) shows the typical PL decay profiles monitored at $\sim$1.23-eV photon energy at different temperatures under a weak excitation density of $\sim$4 μJ/cm^2. The observed PL profiles are non-exponential decays and well reproduced by a sum of three exponentials, $I(t) = I_1 \exp(-t/\tau_1) + I_2 \exp(-t/\tau_2) + I_3 \exp(-t/\tau_3)$ as shown by the dashed lines. The origin of each component remains unclear. A common way to evaluate the carrier lifetime in complicated systems like CZTS is using the mean decay time. The mean decay time, determined as $\langle\tau\rangle = (I_1\tau_1 + I_2\tau_2 + I_3\tau_3)\ /(I_1 + I_2 + I_3)$, is shown as a function of temperature in Fig. 1(b). At temperatures below 100 K, $\langle\tau\rangle$ is estimated to be in the range of microseconds and decreases slightly with increasing temperature, but at temperatures above 100 K, $\langle\tau\rangle$ decreases rapidly with increasing temperature to a subnanosecond value at RT.

Because CZTS is a direct-gap semiconductor,[1,7] the slow decay times that we observe at low temperatures indicate the localized nature of the photogenerated carriers in the CZTS single crystals. These PL properties are different from those of conventional binary semiconductor compounds. Shortly after laser excitation, photocarriers are nonradiatively captured in spatially separated band tails, where the origins of the band tail states are the statistical potential fluctuations caused by the composition of quaternary crystals and the electrostatic potential fluctuations caused by the charged impurities and defects in CZTS.[3,13–16,24] Because thermal energies at low temperatures are insufficient, the majority of the captured carriers cannot cross the potential barriers into the conduction or valence bands and are, therefore, well localized in the ground states of the band tails. This means that radiative recombination of the localized carriers occurs through variable-range hopping motions[16,20,21] resulting in the long microsecond-scale mean decay time $\langle\tau\rangle$. At temperatures above 100 K, however, the temperature dependence of $\langle\tau\rangle$ can be described approximately by the Arrhenius equation

$$\langle\tau\rangle = \tau_0[1 + C\exp(-E_a/k_BT)]^{-1}, \quad (1)$$

where E_a is the activation energy, and τ_0 and C are constants. The temperature dependence of $\langle\tau\rangle$ with $E_a = 112 \pm 16$ meV is shown by the solid line in Fig. 1(b). Theoretical calculations have predicted the Cu_{Zn} antisite is the most dominant acceptor defect in CZTS as it has the lowest formation energy.[5,6] The energy difference between the Cu_{Zn} acceptor level and the valence band maximum was calculated theoretically to be $\sim$120 meV,[6] which is very similar to our experimental value. Thus, we assigned the $\sim$112-meV activation energy to the average potential depth of the acceptor band tails.[20]

The considerable decrease in $\langle\tau\rangle$ at high temperatures implies significant enhancement of the nonradiative recombination processes; at high temperatures, some of the carriers localized to the band tails are released thermally to the conduction and valence bands, and these released carriers are likely to be involved in nonradiative processes within a short time. The quaternary composition of CZTS is such that a large number of nonradiative sites are formed naturally,[5,6] thus promoting the efficient and rapid nonradiative capture of the thermally released carriers in the conduction and valence bands. Moreover, we note that the carrier density increases considerably as the temperature increases, consequently resulting in metal-like behavior at RT being observed in temperature-dependent Hall measurements.[20] Hence, in addition to single-carrier trapping to nonradiative sites, nonradiative Auger recombination might occur, similar to the situation in heavily doped semiconductors.[22,23] The significant change of $\langle\tau\rangle$ of nearly four orders of magnitude (microseconds at 10 K to subnanoseconds at RT) is strong indication that nonradiative recombination at high temperatures in CZTS single crystals is drastically enhanced.

The results of the steady-state PL measurements shed more light on the band tail states and nonradiative recombination processes. Figure 2(a) shows PL spectra at different temperatures under an excitation density of $\sim$4 μJ/cm^2. Based on the excitation density dependence of the steady-state PL spectrum, we concluded that the PL originates from the band tail states of CZTS.[3] The broad spectral width of the PL band is considered to be determined primarily by the inhomogeneous broadening originating from the distribution of the band-tail density. The PL peak energies, obtained from Gaussian fits and shown as a function of temperature in Fig. 2(b), reveal a blueshift of $\sim$45 meV as the temperature increases from 10 K to RT. A similar temperature dependence of the PL peak energy was recently reported for CZTS single crystals and polycrystalline thin films;[9,14,15] and this increase in the PL peak energy can be explained

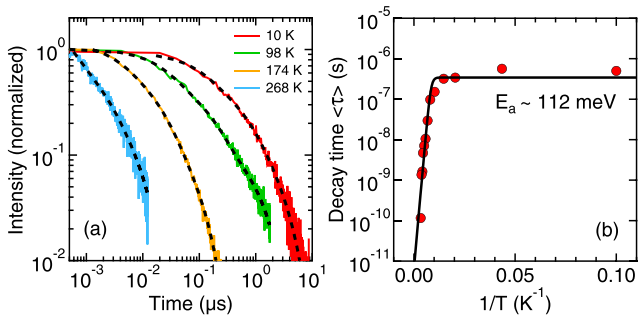

FIG. 1. (a) Log-log plots of typical PL decay profiles of the monitored photon energy $\sim$1.23 eV at different temperatures measured under a weak excitation density of $\sim$4 μJ/cm^2. The dashed lines show the three-exponential-component fits. (b) The mean decay time $\langle\tau\rangle$ as a function of temperature. The solid black line is the fitting result given by Eq. (1).

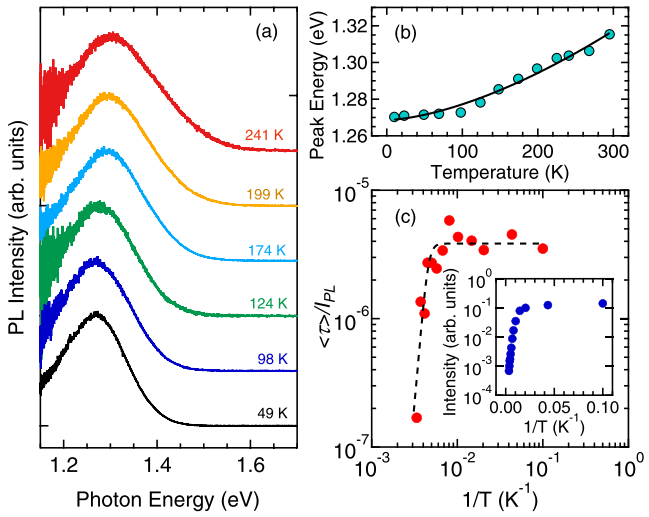

FIG. 2. (a) PL spectra at different temperatures (shifted vertically for clarity) under a weak excitation density of ~4 μJ/cm^2. (b) The PL peak energy as a function of temperature. The solid line is a guide for the eye. (c) Log-log plot of the temperature dependence of $\langle\tau\rangle/I_{PL}$ which is proportional to the radiative lifetime of the photogenerated carrier τ_{rad}. The dashed line is a guide for the eye. The inset is the temperature dependence of the time-integrated PL intensity I_{PL}.

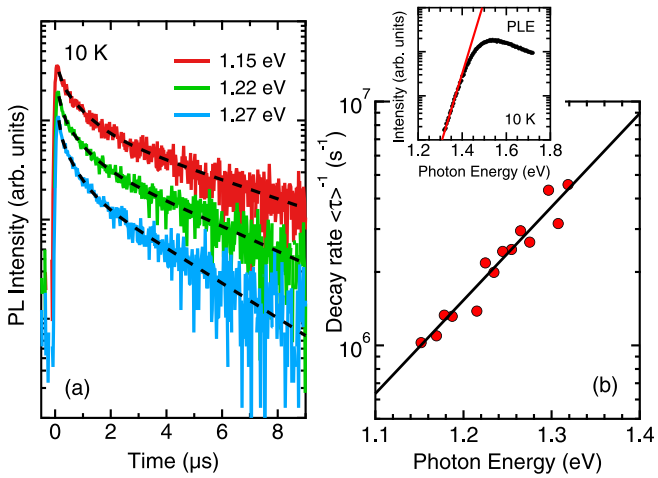

FIG. 3. (a) Typical PL decay profiles of different monitored PL photon energies (shifted vertically for clarity) measured under a fairly weak excitation density of ~0.4 μJ/cm^2 at 10 K. The dashed lines show the three-exponential-component fits. (b) Semi-log plot of the PL-photon-energy dependence of the mean decay rate $\langle\tau\rangle^{-1}$ at 10 K. The solid black line shows the exponential fitting result. The inset is a semi-log plot of the PL excitation spectrum measured at 10 K. The solid red line is the exponential fit of the low-energy tail.

using the potential fluctuation model (the formation of band tail states).[14–16,24] In the view point of the potential fluctuation model, the energy shift of the PL peak depends strongly on the density of the tail states in the CZTS samples.[14–16] The observed blueshift of the PL peak energy indicates the existence of band-tail states with a large density of states (DOS).

The inset of Fig. 2(c) shows the time-integrated intensity of the PL band as a function of temperature measured under an excitation density of ~4 μJ/cm^2. As the temperature increases from 10 K to RT, the time-integrated PL intensity I_{PL} exhibits a decrease of about two orders of magnitude, far smaller than that of the mean decay time $\langle\tau\rangle$. Note that the PL intensity I_{PL} can be estimated as $I_{PL} \sim \langle\tau\rangle/\tau_{rad}$, where τ_{rad} is the radiative lifetime of the photogenerated carriers. The observed discrepancy between the temperature dependences of the PL intensity I_{PL} and mean decay time $\langle\tau\rangle$, therefore, indicates a temperature dependence of the radiative lifetime τ_{rad}. A log-log plot of the temperature dependence of $\langle\tau\rangle/I_{PL}$, which is proportional to the radiative lifetime τ_{rad}, is shown in Fig. 2(c). At temperature below 100 K, τ_{rad} is almost constant, but at temperatures above 100 K, τ_{rad} decreases with increasing temperature, and at RT, it reaches a value estimated to be about one order smaller than that at low temperatures. This temperature dependence of the radiative lifetime τ_{rad} means the radiative recombination process at low temperatures is different from that near RT. The radiative recombination process at low temperatures is determined primarily by variable-range hopping motion of the photogenerated carriers,[16,20,21] whereas thermally activated multiple trapping process takes an important role in the radiative recombination process at RT.[3,25]

To investigate the photocarrier recombination dynamics in the tail states below the band edge, we examined the mean decay rate $\langle\tau\rangle^{-1}$, which depends strongly on both the PL photon energy and excitation density. Figure 3(a) shows typical decay profiles of different PL energies at 10 K under a fairly weak excitation density of ~0.4 μJ/cm^2; the dashed lines are fits using the three-exponential-component equation noted earlier. The PL-photon-energy dependence of the mean decay rate $\langle\tau\rangle^{-1}$ (Fig. 3(b)) shows that $\langle\tau\rangle^{-1}$ exhibits an exponential dependence on the PL photon energy. A log-log plot of the PLE spectrum measured at 10 K (Fig. 3(b), inset) reveals a long exponential tail near the band edge (solid red line) in the PLE spectrum, indicating that the density of the band tails in CZTS single crystals has an exponential distribution.[26–28] The exponential dependence of $\langle\tau\rangle^{-1}$ at 10 K is believed to be due mainly to this exponential distribution of the band-tail-state density.[27,28] In addition, the observed increase in $\langle\tau\rangle^{-1}$ with the PL photon energy may be connected to the fact that the recombination of carriers localized in nearby band tails have a larger decay rate, as well as a higher emission photon energy than the recombination of carriers localized in distant band tails.[11]

Typical PL decay profiles of the emission energy of ~1.23 eV under different excitation densities at 10 K are shown in Fig. 4(a) along with fits of the data, and Figure 4(b) shows the mean decay rate $\langle\tau\rangle^{-1}$ at 10 K as a function of excitation density. Under low excitation densities, the photogenerated carriers are localized near the lowest energy state of the band tails. As the excitation density increases, the trapped carriers tend to occupy higher-energy states with a larger band-tail DOS, which consequently leads to an increase in $\langle\tau\rangle^{-1}$ and a blueshift of the PL peak energy (consistent with the steady-state PL measurement results; data not shown). In addition, with an increase in the excitation density, the average spatial distance among the photogenerated carriers is reduced, leading to an increase in $\langle\tau\rangle^{-1}$.[11] The excitation density dependence of the time-integrated PL intensity, also shown in Fig. 4(b), indicates a change from a linear dependence (solid black line) to a sublinear dependence (that tends toward saturation) that signals a decrease in the PL efficiency under strong excitation densities. Therefore, it is possible that nonradiative Auger recombination partly contributes to the increase in $\langle\tau\rangle^{-1}$ in the strong-excitation-density regime.[22]

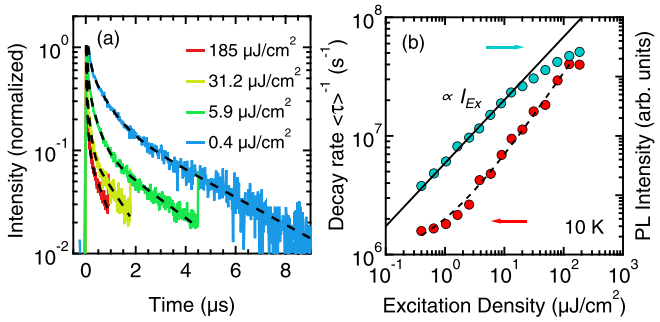

FIG. 4. (a) Typical PL decay profiles of the emission energy ~1.23 eV under different excitation densities measured at 10 K. The dashed lines show the three-exponential-component fits. (b) Log-log plots of the excitation-density dependence of the mean decay rate $\langle\tau\rangle^{-1}$ (solid red circles) and of the time-integrated PL intensity (solid blue circles) at 10 K. The dashed line is a guide for the eye. The solid line is the linear fit of the PL intensity in the weak excitation region.

Finally, we give a brief comment about effects of drastically enhanced nonradiative recombination at high temperatures on the performance of CZTS-based solar cells. Drastically enhanced nonradiative recombination including quick capture at nonradiative sites results in the very short picosecond lifetime of the mobile carriers at high temperatures.[3] The short lifetimes in turn lead to very short diffusion lengths of the mobile carriers, estimated roughly to be on the order of nanometers,[29] that limit carrier collection to deep regions in the CZTS absorber layer, and consequently, CZTS-based solar cells present low power conversion efficiencies.

In conclusion, we have determined the temperature dependence of photocarrier recombination dynamics in CZTS single crystals. At low temperatures, localization of the photocarriers to the band tails results in microsecond decay time. However, nonradiative recombination becomes dominant at high temperatures, and consequently a considerable decrease of four orders of magnitude of the PL decay time was observed along with significant quenching of the PL intensity. These fast nonradiative recombination processes will have a strong influence on the power conversion efficiency of CZTS-based solar cells. Our results, therefore, provide essential knowledge for further improving the performance of CZTS-based solar cells.

This work was supported by JST-CREST and the Sumitomo Electric Industries Group CSR Foundation.

[1]K. Ito and T. Nakazawa, Jpn. J. Appl. Phys., Part 1 **27**, 2094 (1988).
[2]H. Katagiri, K. Jimbo, W. S. Maw, K. Oishi, M. Yamazaki, H. Araki, and A. Takeuchi, Thin Solid Films **517**, 2455 (2009).
[3]L. Q. Phuong, M. Okano, Y. Yamada, A. Nagaoka, K. Yoshino, and Y. Kanemitsu, Appl. Phys. Lett. **103**, 191902 (2013).
[4]B. Shin, O. Gunawan, Y. Zhu, N. A. Bojarczuk, S. J. Chey, and S. Guha, Prog. Photovoltaics **21**, 72 (2013).
[5]A. Nagoya, R. Asahi, R. Wahl, and G. Kresse, Phys. Rev. B **81**, 113202 (2010).
[6]S. Chen, J. H. Yang, X. G. Gong, A. Walsh, and S. H. Wei, Phys. Rev. B **81**, 245204 (2010).
[7]C. Persson, J. Appl. Phys. **107**, 053710 (2010).
[8]T. Gershon, B. Shin, T. Gokmen, S. Lu, N. Bojarczuk, and S. Guha, Appl. Phys. Lett. **103**, 193903 (2013).
[9]K. Tanaka, Y. Miyamoto, H. Uchiki, K. Nakazawa, and H. Araki, Phys. Status Solidi A **203**, 2891 (2006).
[10]Y. Miyamoto, K. Tanaka, M. Oonuki, N. Moritake, and H. Uchiki, Jpn. J. Appl. Phys., Part 1 **47**, 596 (2008).
[11]T. Gershon, B. Shin, N. Bojarczuk, T. Gokmen, S. Lu, and S. Guha, J. Appl. Phys. **114**, 154905 (2013).
[12]S. Levcenko, V. E. Tezlevan, E. Arushanov, S. Schorr, and T. Unold, Phys. Rev. B **86**, 045206 (2012).
[13]J. P. Leitao, N. M. Santos, P. A. Fernandes, P. M. P. Salome, A. F. da Cunha, J. C. Gonzalez, G. M. Ribeiro, and F. M. Matinaga, Phys. Rev. B **84**, 024120 (2011).
[14]M. J. Romero, H. Du, G. Teeter, Y. Yan, and M. M. Al-Jassim, Phys. Rev. B **84**, 165324 (2011).
[15]D. P. Halliday, R. Claridge, M. C. J. Goodman, B. G. Mendis, K. Durose, and J. D. Major, J. Appl. Phys. **113**, 223503 (2013).
[16]T. Gokmen, O. Gunawan, T. K. Todorov, and D. B. Mitzi, Appl. Phys. Lett. **103**, 103506 (2013).
[17]Y. Yamada and Y. Kanemitsu, Appl. Phys. Lett. **101**, 133907 (2012).
[18]A. Nagaoka, K. Yoshino, H. Taniguchi, T. Taniyama, and H. Miyake, J. Cryst. Growth **341**, 38 (2012).
[19]T. K. Todorov, K. B. Reuter, and D. B. Mitzi, Adv. Mater. **22**, E156 (2010).
[20]A. Nagaoka, H. Miyake, T. Taniyama, K. Kakimoto, and K. Yoshino, Appl. Phys. Lett. **103**, 112107 (2013).
[21]V. Kosyak, M. A. Karmarkar, and M. A. Scarpulla, Appl. Phys. Lett. **100**, 263903 (2012).
[22]H. Yasuda and Y. Kanemitsu, Phys. Rev. B **77**, 193202 (2008).
[23]Y. Yamada, H. Yasuda, T. Tayagaki, and Y. Kanemitsu, Phys. Rev. Lett. **102**, 247401 (2009).
[24]A. P. Levanyuk and V. V. Osipov, Sov. Phys. Usp. **24**, 187 (1981).
[25]T. Tiedje and A. Rose, Solid State Commun. **37**, 49 (1981).
[26]D. L. Wood and J. Tauc, Phys. Rev. B **5**, 3144 (1972).
[27]Y. Kanemitsu, Phys. Rev. B **49**, 16845 (1994).
[28]Y. Kanemitsu, Phys. Rev. B **53**, 13515 (1996).
[29]O. Gunawan, T. K. Todorov, and D. B. Mitzi, Appl. Phys. Lett. **97**, 233506 (2010).